CSD-2019 Special Issue

J. Indian Chem. Soc.,
Vol. 97, No. 12c, December 2020, pp. 2889-2896

Photodegradation of Congo Red using Cu^{2+} engrafted $MgAl_2O_4$ nanoparticles under Solar irradiation

Arnab Mukherjee and Debasis Dhak*

Nanomaterials Research Lab, Department of Chemistry, Sidho-Kanho-Birsha University, Purulia-723 104, West Bengal, India

E-mail: debasisdhak@yahoo.co.in

Manuscript received online 04 December 2020, revised and accepted 24 December 2020

Nanosized, pH stable, Cu^{2+} engrafted $MgAl_2O_4$ ($Mg_{1-x}Cu_xAl_2O_4$, x = 0, 0.3 abbreviated as MCA0, and MCA3 respectively), have been synthesized chemically and the cubic phase of the nanoparticles was estimated from the X-ray diffraction (XRD) and transmission electron microscopy analysis (TEM). The bandgap energies, grain size, effective radius into an aqueous medium, and the zero-point charge (pH_{ZPC}) were appraised by diffuse reflectance spectra (DRS), scanning electron microscope (SEM), dynamic light scattering (DLS) study, and ξ-potential analysis respectively. MCA3 (specific surface area 22.14 m^2/g) with 98.17% photodegradation for 10^{-5} (*M*) CR solution obeying pseudo-first order kinetics and reusable up to 4 cycles at pH 7. The photodegradation mechanism was postulated by the UV, FTIR, and high-performance liquid chromatography (HPLC) analyses.

Keywords: Photocatalyst, dynamic light scattering (DLS) study, kinetics, high-performance liquid chromatography (HPLC).

Introduction

Congo Red (CR) [1-naphthalene sulfonic acid, 3,3′-(4,4′-biphenylenebis(azo)bis(4-amino-)disodium] with two -N=N- chromophores is a class of azo dye which is not readily degradable, highly toxic, even carcinogenic and due to environmental problems, it has been banned in many countries[1]. However, the traditional physical, chemical, and biological treatments often have a slight degradation effect on this diazo pollutant due to the aromatic structures providing physico-chemical, thermal and optical stability[2]. Therefore, an urgent requirement is needed to develop a low-cost process to degrade or mineralize the dye molecules.

TiO_2[3], zeolite[4], $Ni(OH)_3$ and NiO[5], Fe_2O_3[6], CeO_2[7], carbon nanotubes[8], CdS[1], $Zn_{1-x}Cu_xS$ and $Zn_{1-x}Ni_xS$[9], ZnO[10] were also used as photocatalysts due to narrow band high with photocatalytic degradation property. $MgAl_2O_4$, a typical spinel material (Mg^{2+} occupy tetrahedral sites, and Al^{3+} in octahedral site) has a vast applications such as ceramic capacitor, humidity sensors, and catalyst/catalyst support, etc.[11]. Recently, Ismail *et al.*, reported nanosized $MgAl_2O_4$ nanoparticles synthesized by coprecipitation methods, for the degradation of methylene blue[12]. Muneeb *et al.*, removed of methyl orange photo-catalytically by $MgAl_2O_4$-Sb_2S_3 composite[13]. From an economic point of view, the 3d transition metals catalysts[14] such as copper to prepare composite for high activity at low-temperature and with lower bandgap (E_g = 1.9 eV)[15].

We investigate the photocatalytic property of Cu^{2+} engrafted $MgAl_2O_4$ nanoparticles with general chemical formula $Mg_{1-x}Cu_xAl_2O_4$ (x = 0, 0.3) abbreviated as MCA0 and MCA3 synthesized by the solution combustion method using triethanolamine (TEA)[16], to photodegrade of water-soluble carcinogenic dye CR using Solar irradiation.

Experimental

Materials and methods

Materials:

During the experiments, the chemicals required were $Mg(OAc)_2.4H_2O$ (98–102%), $Cu(NO_3)_2.3H_2O$ (≥99%), $Al(NO_3)_3.9H_2O$ (≥95%), TEA (≥99%), CR, ethanol, HCl, NaOH, HNO_3, and double-distilled water (chemicals purchased from the Merck Specialties Limited, Mumbai).

Methods:

Preparation of $Mg_{1-x}Cu_xAl_2O_4$ (x = 0, 0.3) photocatalysts:

$Mg_{1-x}Cu_xAl_2O_4$ (x = 0, 0.3) abbreviated as MCA0 and MCA3 have prepared using the solution combustion method using TEA as discussed in the previous communication[16].

Characterization:

The thermogravimetric analysis (TGA) (Perkin-Elmer STA 6000) was done from 30°C to 800°C at heating rate 10°C/min using α-alumina as a standard in N_2 atmosphere. The UV-Vis studies were done using LAMBDA35, Perkin-Elmer, UK. The dynamic light scattering (DLS) investigation was done using Malvern Zetasizer Nano ZS90 (United Kingdom). The specific surface area was determined by the N_2 adsorption/desorption method at a liquid N_2 temperature of 77.350 K using NOVA touch 4LX (F/W ver. 1.05, Serial# 17018101901), Quanta chrome, USA. The pH measurements were done using Thermo Scientific (Orion Versa star Pro) Advance Electrochemistry Meter (Software Revision: r4.06, serial number: V11855). The high-performance liquid chromatography (HPLC), of CR and its photodegraded products, were done using UHPLC 3000, Thermo Scientific (United States) with Thermo Scientific Hypersil GOLD aQ, Part No. 25303-154630 (150×4.6 mm) column with 3 µ particle size, mobile phase consisted of acetonitrile/water (70:30 v/v%) for CR and the flow rate was set 1.0 mL/min. Approximately 25 µL volume of samples were injected in the column and the effluent was monitored at 497 nm.

Results and discussion

Physicochemical characterization:

The thermal degradation occurred in three stages as shown in Fig. 1, with an overall mass loss of 56.26% and 59.88% for MCA0 and MCA3 respectively. In Stage I, ~200°C 13.40% and 11.13% of mass loss were observed due to the adsorbed water, for MCA0 and MCA3 respectively. The second weight loss with 49.50% occurred between 200°C–450°C, with the elimination of CO_2, NH_3, and nitrogenous oxide in Stage II. In Stage III, at >500°C, a gradual decrease of mass with complete volatilization and the sample tended to reach its calcination temperature with a weight loss of 12.90% and 11.39%. The TG graph paralleled with the X-axis above 600°C and that is why, calcination was performed at 700°C to get the desired phase. The detailed mechanism has been discussed by Dhak *et al.*[17].

The detailed analysis of XRD, FTIR, SEM, TEM, bandgap (E_g ev), and pH_{ZPC} studies of MCA are discussed in our pre-

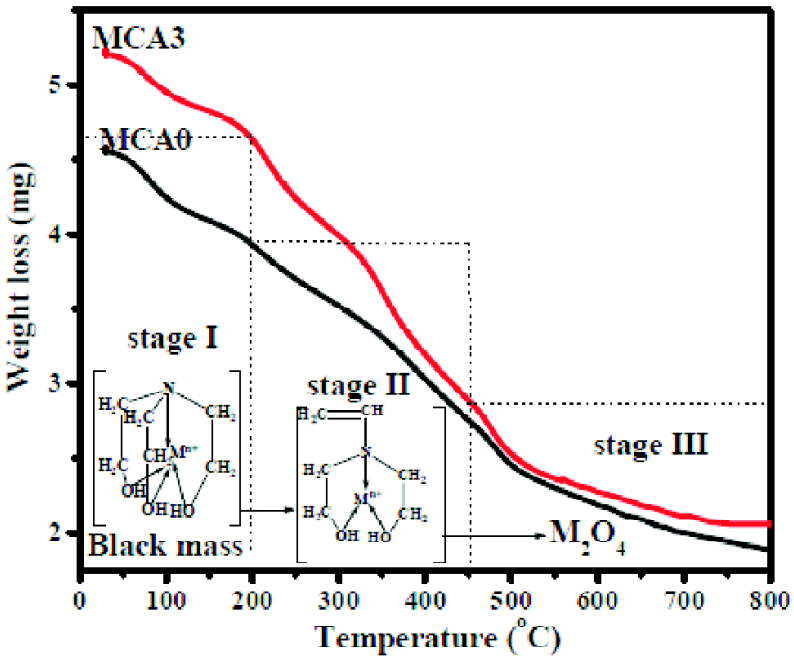

Fig. 1. Thermogravimetric analysis (TGA) of MCA.

vious communication[16]. The radius of MCA3 in aqueous medium was between 50±1.12 nm obtained from the DLS study as shown in Fig. 2a which represents the formation of hydrated MCA3 moiety and thus the particle size (TEM size = 42.68±1.11 nm) increased. The typical N_2 adsorption-desorption isotherm for the MCA3 is shown in Fig. 2b where nearly Type I Brunauer-Emmett-Teller isotherm (BET) indicating microporous nature of the sample[18]. The specific surface area and pore volume were 22.14 m^2/g, and 0.623 cc/g respectively. The pore size distribution plot using the Barrett-Joyner-Halenda (BJH) method and the average pore radius of MCA3 was 1.82 nm is shown in Fig. 2b (inset).

Photocatalytic study

A 1000 mL 10^{-5} (*M*) CR solution was made by dissolving the required quantity of CR in double-distilled water and from that stock solution, 100 mL solution were taken in 250 mL glass beaker and mixed with 4 mmol MCA and stored in dark for 30 min to establish the adsorption/desorption equilibrium as per the reported work[16]. The decolorization along with the photocatalytic degradation of CR using MCA was confirmed by the UV-Vis spectral study using the arresting solutions (3 mL) taken. The absorption spectra of CR continuously decreased with increase in the irradiation time from the maximum absorption peak i.e., 497 nm (visible region) and 344 nm (ultraviolet region) respectively[1] and finally paralleled with the X-axis indicating the complete degradation as shown in Fig. 3a and 4a for MCA0 and MCA3 respectively. The total time required for the photodegradation of CR using MCA0 and MCA3 was 210 min and 120 min with 80.66% and 98.17% degradation respectively calculated using standard equation[19] at pH 7.

Kinetic study

The variation in the concentration with the prolonged irradiation time was recorded as shown in Fig. 3b, 4b for MCA0 and MCA3 respectively and the set without MCA showed no such degradation. The reaction kinetics obeyed the Lindemann-Hinshelwood pseudo-first order kinetics[20] as shown in Fig. 3c and 4c with rate constant (k_1) values 1.25×10^{-4} s^{-1} and 2.03×10^{-4} s^{-1} for MCA0 and MCA3 respectively. The k_1 value and the regression coefficient (R^2 = 0.988) for MCA3 were greater and close to unity than the MCA0 so the pH variation and effect of different inorganic anions (NO_3^-, Cl^-, SO_4^{2-}) in the CR photodegradation process were continued with MCA3.

pH study, the effect of co-ions, and reuse study

Solution pH has a strong effect on the photodegradation performance[1] and the anionic azo dye CR shows different equilibrium in the lower (pH < pH_{ZPC}) and higher pH (pH > pH_{ZPC}) as shown in Fig. 5a. The pH_{ZPC} of MCA3 was found

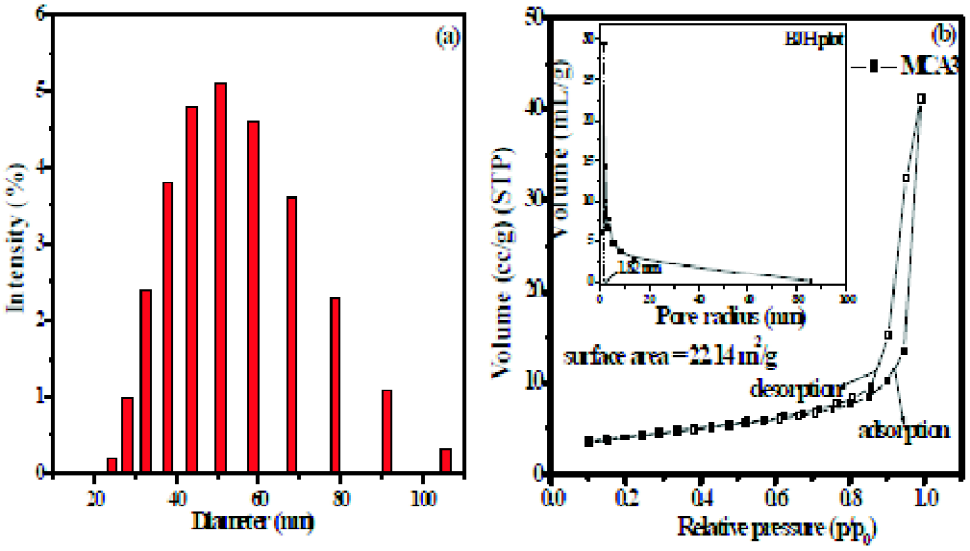

Fig. 2. (a) Dynamic light scattering study (DLS) and (b) N_2 adsorption-desorption isotherm for the MCA3 (inset: BJH plot) calcined at 700°C for 3 h.

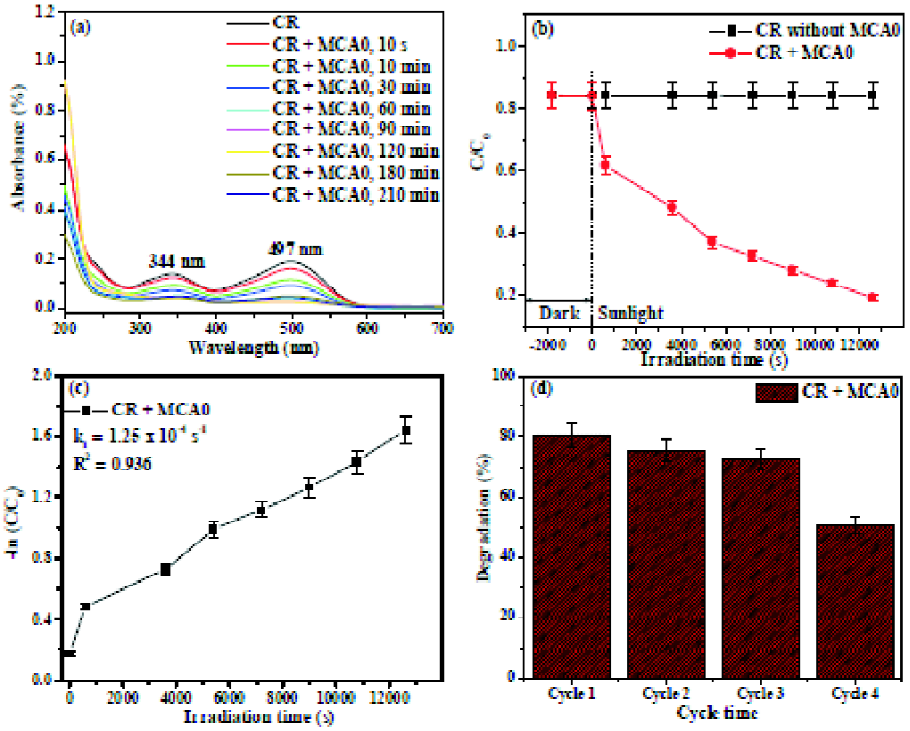

Fig. 3. (a) UV-Vis absorbance spectra of 10^{-5} (*M*) CR solution, (b) change in concentration of CR under solar irradiation, (c) pseudo-first order kinetic plot and (d) reuse study of photodegradation using MCA0 calcined at 700°C for 3 h.

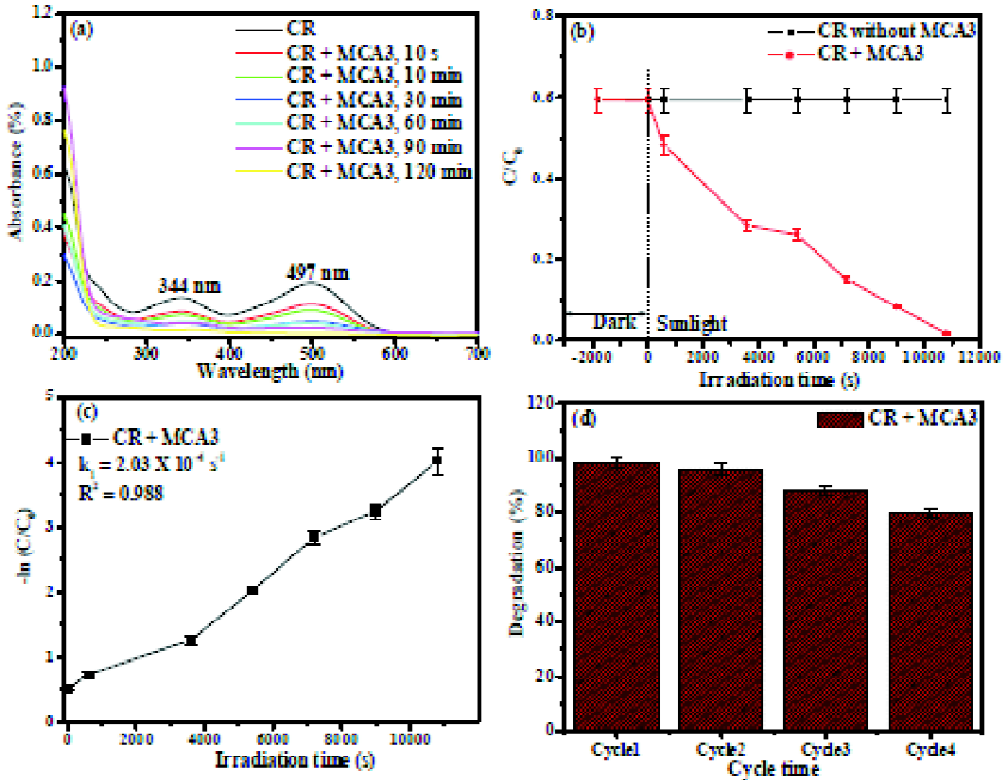

Fig. 4. (a) UV-Vis absorbance spectra of 10^{-5} (*M*) CR solution, (b) change in concentration of CR under solar irradiation, (c) pseudo-first order kinetic plot and (d) reuse study of photodegradation using MCA3 calcined at 700°C for 3 h.

to be 8.8[16] and thus in the lower pH region (pH < 7) due to the positively charged surface of MCA3 the interaction of CR with MCA3 increased leading to higher degradation (98.66%) at lower pH 2. The degradation of CR got decreased (80.23%) at the higher pH medium (pH 11) due to an increase in the OH^- ions in the medium leading to less interaction with the anionic dye as the MCA3 surface was negatively charged at pH > pH_{ZPC}. The CR photodegradation kinetics in different pH mediums also obeyed the pseudo-first order kinetics (R^2 = 0.955) as shown in Fig. 5a (inset).

As there are large amounts of negative ions, especially NO_3^-, SO_4^{2-}, and Cl^- present in wastewater of textile and dye industries[1] thus to investigate the influence of these anions on photocatalytic degradation of CR 0.01 (*M*) of the corresponding sodium salts were mixed into the 10^{-5} (*M*) CR solution and irradiated into Sunlight with 4 mmol MCA3 and the effect of Na^+ neglected[21]. The variation in the concentration of CR in presence of co-ions in the photodegradation was shown in Fig. 5b and the kinetics obeyed the pseudo-first order kinetics as shown in Fig. 5c. The degradation improved in the presence of NO_3^- which was discussed in the mechanism section. In the presence of SO_4^{2-}, and Cl^- the degradation noticeably decreased as shown in Fig. 5d as the competition with the anions dye CR with the MCA3 surface increased. MCA0 and MCA3 were successfully reused up to 4 cycles using previously reported regeneration process[16] as shown in Fig. 3d and Fig. 4d respectively where MCA3 shows higher efficiency than MCA0.

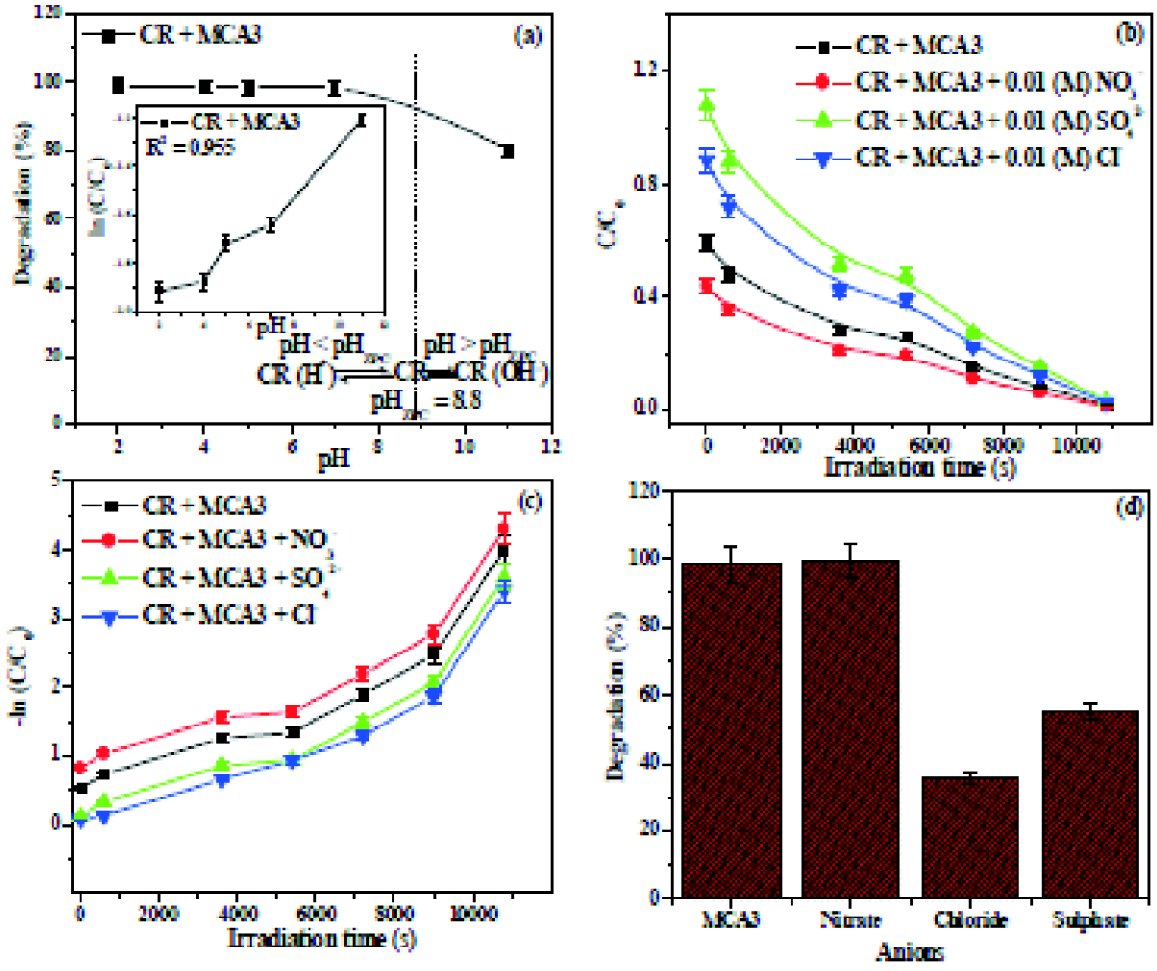

Fig. 5. (a) pH variation study, (b) change in concentration of CR, (c) pseudo-first order kinetic plot and (d) degradation of CR using MCA3 in presence of NO_3^-, SO_4^{2-}, and Cl^-.

Mechanistic study

The photocatalytic activity depends on the photogenerated electrons (e^-_{CB}), holes (h^+_{VB}) and the OH• upon Solar irradiation[2]. To find out the role of e^-_{CB}, h^+_{VB} and OH• to the photodegradation of CR was performed in the presence of different scavenges[22] and OH• has a key role in this degradation process as the degradation decreased abruptly in presence of OH• scavenger isopropyl alcohol (IPA) as shown in Fig. 7c. Thus, the following mechanism could be proposed as stated in eqs. ((1)-(3)).

$$MCA + hv \rightarrow h^+_{VB} + e^-_{CB} \quad (1)$$

$$H_2O + h^+_{VB} \rightarrow H^+ + OH^\bullet \quad (2)$$

$$CR + OH^\bullet \rightarrow \text{mineralization } (CO_2 + H_2O) \quad (3)$$

In the presence of NO_3^- the generation of the accelerated as shown in eq. (4) leading to an increase in degradation as shown in Fig. 5b, c.

$$NO_3^- + H_2O + hv \rightarrow NO_2^- + OH^- + OH^\bullet \quad (4)$$

The mineralization of CR was explained by the UV, FTIR and the HPLC studies. Under the Solar irradiation, MCA produces h^+_{VB} in the valance band (VB) and e^-_{CB} in the conduction band (CB) as shown in the diagram Fig. 6.

Holes (h^+_{VB}) interacts with the water molecules to generate OH• and the OH• attacks the CR leading to rupture the azo bond as well as the aromatic rings. Thus, the absorption band at 497 nm for the azo group and 344 nm for the benzene naphthalene ring decreased and finally paralleled with the X-axis as shown in the UV studies (Figs. 3a, 4a)[1]. The FTIR study of the CR photodegradation using MCA3 is shown in Fig. 7a. For CR [Fig. 7a(a)] the peaks at 651–547 cm^{-1} showed the C–C bending and 702 cm^{-1} for C–H stretching vibrations of disubstituted CR[23]. The peaks at 846–750 cm^{-1} and 1068 cm^{-1} were for the *para*-substituted ring substitution vibrations and S=O stretching vibrations of the sulphonic acid respectively[24]. The band at 1183 cm^{-1} is mainly for the multi-substituted aromatic ring and 1234 cm^{-1}, 1356 cm^{-1} represent the C–N stretching and bending vibrations[25] present in CR respectively. The peaks at 1449 cm^{-1} and 1608 cm^{-1} were for the aromatic C=C and N=N stretching vibrations[23]. The peaks at 3240 cm^{-1} and 3427 cm^{-1} were for the O–H stretching and N–H stretching of the aromatic primary amine group[23] respectively. In FTIR study as shown in Fig. 7a(b) it was evident that in the final aliquot, there were no such characteristic peaks of CR (especially from 846–547 cm^{-1}) indicating the disappearance of the corresponding groups (C–C bending, C–H stretching, *para*-substitutions, and S=O stretching, etc.) present in CR. The lowering of the peaks at 1449–1068 cm^{-1} confirmed the vanishing of aromatic C=C stretching, C–N bending, and stretching vibrations respectively. In the final aliquot, the peak for the O–H and N–H stretching of aromatic 1° amine got disappeared and broadened revealed the degradation of CR photo-catalytically using MCA3 in Solar irradiation[26]. The stability of the MCA3 after the photocatalytic test was checked by the FTIR analysis as shown in Fig. 7c were no typical peaks of CR present

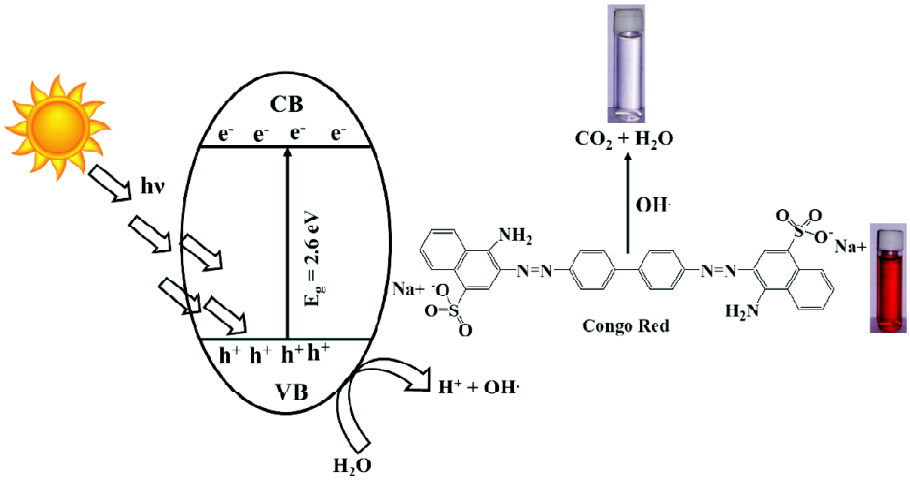

Fig. 6. Diagram of the photodegradation of CR using MCA3 under Solar irradiation.

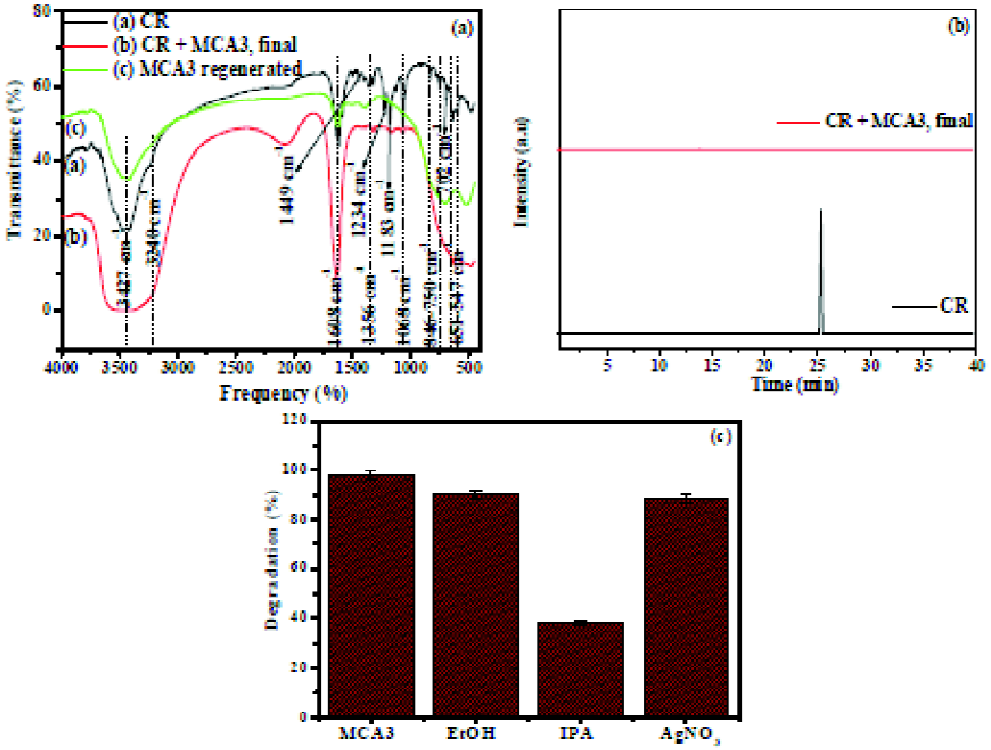

Fig. 7. (a) FTIR analysis, (b) HPLC analysis of CR using MCA3 and (c) photodegradation of CR using MCA3 in presence of 0.05 mM trapping agents as mentioned under Solar irradiation.

in the FTIR spectrum of the regenerated MCA3. The HPLC study of the photodegradation process completely established the mineralization phenomenon as shown in Fig. 7b. CR shows HPLC peak at 25.35 min (R_t = 25.35 min)[27] and the HPLC of the final aliquot became parallel with the X-axis emphasizing the rupture of aromatic rings, cleavage of various C–C, C=C, C–N bonds, and aromatic structures to form CO_2 and H_2O as the final product.

Conclusion

Cu^{2+} engrafted MCA nanocomposites were prepared by solution combustion method using triethanolamine (TEA) and applied for the photodegradation of the aqueous CR solution at pH 7 under Solar irradiation. The degradation of MCA0 and MCA3 was 80.66% and 98.17% at pH 7 respectively. The degradation kinetics obeyed the pseudo-first order kinetics (Lindemann-Hinshelwood model) and the rate constants were in 10^{-4} s^{-1} order. Hydroxyl radical ($OH^{\bullet}$) has a vital role in photodegradation established from the $OH^{\bullet}$ trapping experiment using 0.05 mM IPA solution. It has been found that the solution pH and the co-existing anions (NO_3^-, SO_4^{2-}, and Cl^-) influenced the photocatalytic degradation of CR. The presence of NO_3^- the degradation accelerated as it increased the concentration in the reaction medium but in presence of SO_4^{2-}, and Cl^- the degradation inhibited as the repulsion increased, and competition with anionic dye CR with the MCA3 surface. UV-Vis, FTIR, and HPLC analysis were applied to demonstrate the photodegradation of CR using MCA3 under Solar irradiation. MCA3 with 22.14 m^2/g specific surface area could be reused for the photodegradation of CR up to four successive cycles.

Acknowledgements

Authors would like to thank Department of Science and Technology, Government of West Bengal vide project sanction (No. 674(sanc)/ST/P/S&T/15G/5/2016) dated 09/11/2016 for financial support.

References

1. R. J. Huayue Zhu, Ling Xiao, Yuhua Chang, Yujiang Guan, Xiaodong Li and Guangming Zeng, *J. Hazard. Mater.*, 2009, **169**, 933.
2. Y. C. Shuyang Liu, Xiaoyan Cai, He Li, Fei Zhang, Qiuying Mu,

Yongjun Liu and Yude Wang, *Appl. Catal. A: General*, 2013, **453**, 45.

3. D. S. d. S. M. T. C. Sansiviero, A. E. Job and R. F. Aroca, *J. Photochem. Photobiol. A: Chem.*, 2011, **220**, 20.
4. P. K. A. K. Kondru and S. Chand, *J. Hazard. Mater.*, 2009, **166**, 342.
5. Y. L. B. Cheng, W. Q. Cai and J. G. Yu, *J. Hazard. Mater.*, 2011, **185**, 889.
6. R. M. A. Afkhami, *J. Hazard. Mater.*, 2010, **174**, 398.
7. D. Z. Z. X. H. Lu, J. Y. Gan, Z. Q. Liu, C. L. Liang, P. Liu and Y. X. Tong, *J. Mater. Chem. (A),* 2010, **20**, 7118.
8. M. W. L. S. Chatterjee and S. H. Woo, *Bioresour. Technol.*, 2010, **101**, 1800..
9. M. H. K. H. R. Pouretedal, *J. Alloys Compd.*, 2010, **501**, 130.
10. L. N. E. Abdelkader and B. Ahmed, *J. Chem. Eng. Process Technol.*, 2011, **2**, 109.
11. P. Y. Xingzhong Guo, Kazuyoshi Kanamori, Kazuki Nakanishi and Hui Yang, *J. Sol-Gel Sci. Technol.*, 2018, **88**, 114.
12. H. S. Ismail B. and Akram S., *Chem. Eng. J.*, 2013, **219**, 395.
13. I. B. Muneeb M., Fazal T., Khan A. R. and Afzia M., *Recent Pat Nanotechnol.*, 2016, **10**, 213.
14. X. W. S. Hilaire, T. Luo, R. J. Gorte and J. Wagner, *Appl. Catal. (A),* 2001, **215**, 271.
15. J. C. H. X. Wang, J. A. Rodriguez, D. Gamarra, A. Martinez Arias and M. Fernandez-Garcia, *J. Phys. Chem. (B)*, 2006, **110**, 428.
16. A. Mukherjee, M. K. Adak, P. Dhak and D. Dhak, *J. Environ. Sci.*, 2020, **88**, 301.
17. D. Dhak and P. Pramanik, *J. Am. Ceram. Soc.*, 2006, **89**, 1014.
18. M. T. M. Maes, M. Boulhout, S. Schouteden, F. Vermoortele and L. Alaerts, *Angew. Chem. Int. Ed.*, 2011, **50**, 4210.
19. A. Mukherjee, M. K. Adak, S. Upadhyay, J. Khatun, P. Dhak, S. Khawas, U. K. Ghorai and D. Dhak, *ACS Omega*, 2019, **4**, 9686.
20. A. Mukherjee, M. K. Adak, A. Chowdhury and D. Dhak, *Curr. Catal.*, 2019, **8**, 41.
21. K. C. L. G. A. Mohammad and W. M. Ralph, *J. Phys. Chem. (A)*, 1990, **94**, 6820.
22. K. S. A. L. Renuka, Y. S. Vidya, H. P. Nagaswarupa, S. C. Prashantha, S. C. Sharma, H. Nagabhushana and G. P. Darshan, *Appl. Catal. B: Environ.*, 2017, **210**, 97.
23. C. M. S. Satheesh Babu, A. S. Vijayaraj and Mohan A. Dhale, *Ecotoxicology and Environmental Safety*, 2015, **114**, 52.
24. L. M. Zhanying Zhang, Ian M. O'Hara and William O. S. Doherty, *Chem. Eng. J.*, 2011, **178**, 122.
25. R. K. R. Ahmad, *Appl. Surf. Sci.*, 2010, **257**, 1628.
26. S. M. J. A. A. Telke, S. U. Jadhav, D. P. Tamboli and S. P. Govindwar, *Biodegradation*, 2010, **21**, 283.
27. Y. L. Yong-Seok Choi, Min-Ji Kim, Jae-Jin Kim and Gyu-Hyeok Kim, *J. Environ. Sci. and Health, Part A: Toxic/Hazardous Substances and Environmental Engineering*, 2013, **48**, 501.